

Diagnostics possibilities of the solar atmosphere with ALMA interferometer

N. Muratova^{1,2}, A. Berlicki^{1,3}

¹Astronomical Institute, Czech Academy of Sciences, CZECH REPUBLIC,

²Institute of Solar-Terrestrial Physics, SB RAS, RUSSIA, muratova@mail.iszf.irk.ru

³Astronomical Institute, University of Wrocław, POLAND arkadiusz.berlicki@asu.cas.cz

Abstract

Atacama Large Millimeter Array (ALMA) radiointerferometer is the large and complex instrument, which opened the great opportunity to astronomers to investigate physical processes taking place in our Universe and observed at millimeter and submillimeter wavelengths. Due to high sensitivity, very good frequency, temporal and spatial resolution, we can get detailed high-resolution interferometric images of different events, starting from the Sun up to far objects at cosmological distances. Together with investigation of interstellar matter, stars and planet, galaxies, their formation and evolution, ALMA can help to resolve problems of solar physics and allows deeper analysis of solar atmospheric processes. ALMA just started regular solar observations and provides data from an area that has not been available so far. Here, we summarize the capabilities of the instrument and present some examples of diagnostics of different solar structures.

1. SOLAR SCIENCE WITH ALMA

ALMA (Atacama Large Millimeter Array) is located on the Chajnantor plateau at 5000 m altitude consists of 66 antennas, 50 of 12m antenna array, with baselines up to 16 km for high spatial resolution and 12 of 7 m (Compact Array (ACA)) plus 4 of 12 m (Total power Array (TPA)) for wide-field imaging (full disk of the Sun). (<https://almascience.nrao.edu/about-alma/alma-basics>). The wavelengths covered by ALMA range from 0.3 mm to 3.6 mm (frequency coverage of 84 GHz to 950 GHz), depending on transparency windows of atmosphere. At present time, solar observations are possible only in band 3 (84-116 GHz, 2.59-3.57 mm) and band 6 (211-275 GHz, 1.09-1.42 mm) (see Fig. 1). Using ALMA, we can have following opportunities:

1) New spectral diagnostics: possibility of constraining the temperature, density, magnetic field strength, and mass motions in the low solar atmosphere and other cool solar structures.

2) Structure of the low solar atmosphere: analysis of the "temperature minimum" region. By imaging this region of the solar atmosphere at various mm and sub-mm wavelengths, the ALMA will offer a means of characterizing its structure and evolution.

3) Flares: probing the emissions from the most energetic electrons, shedding light on the questions of when, where, and by what mechanism are electrons promptly accelerated to high energies.

4) Filaments and prominences: The observation with ALMA at high spatial resolution will offer for the first time a detailed view of prominence fine structures at mm wavelengths. The measured brightness temperatures in Band 3 and Band 6 will provide the internal temperature structure of the emitting plasma. These measurements will give some additional constraints necessary for theoretical models and related with the energy balance of the cool prominence plasma located within the hot solar corona.

where, and by what mechanism are electrons promptly accelerated to high energies.

4) Filaments and prominences: The observation with ALMA at high spatial resolution will offer for the first time a detailed view of prominence fine structures at mm wavelengths. The measured brightness temperatures in Band 3 and Band 6 will provide the internal temperature structure of the emitting plasma. These measurements will give some additional constraints necessary for theoretical models and related with the energy balance of the cool prominence plasma located within the hot solar corona.

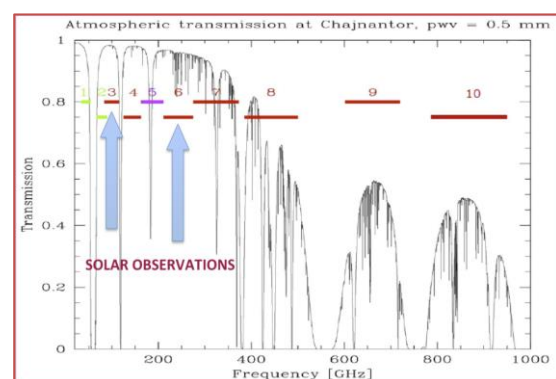


Figure 1. Atmosphere transparency, depending on frequency. Blue arrows mark spectral windows used for solar observations.

Features of observed solar emission in microwave wavelengths give us several advantages. First of all observations of the chromosphere in sub-millimeter/millimeter (SMM) wavelengths are an important diagnostic of its physical conditions. The emission is almost entirely free-free, caused by free electrons colliding with ions and for optically thick features, this emission serves as an excellent thermometer – their brightness being simply proportional to the temperature of emitting gas (Wedemeyer et al. 2016). The opacity is simple, well understood, and is in local thermodynamic equilibrium (LTE) with the electron density. In Fig. 2 heights of different continua formation are represented. Sub-millimeter/millimeter emission is formed in the middle and lower chromosphere and close to the temperature minimum region. In Fig. 3 there is an example of the giant sunspot observation with ALMA interferometer.

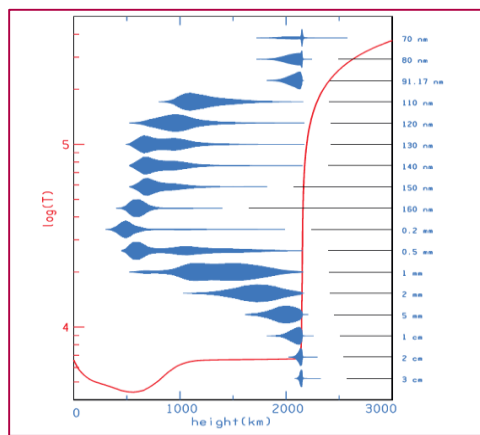


Figure 2. Heights of different continua formation computed for semiempirical C7 model of the solar atmosphere (Avrett and Loeser 2008).

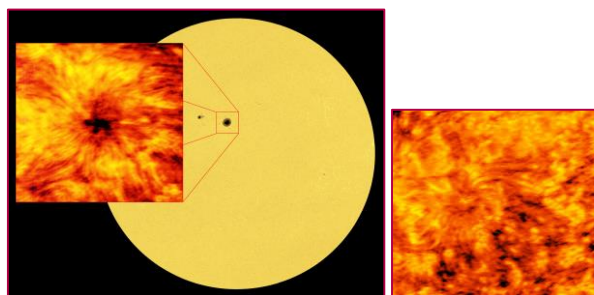


Figure 3. ALMA: giant sunspot with the band 6 receiver at the wavelength of 1.25 mm, acquired on Dec. 18, 2015 – structures similar to H-alpha or Ca II 854.2 nm IR line. (Credit: ALMA (ESO/NAOJ/NRAO))

ALMA can serve also as key to the problem of very high temperature of the solar outer layers (Fig. 4).

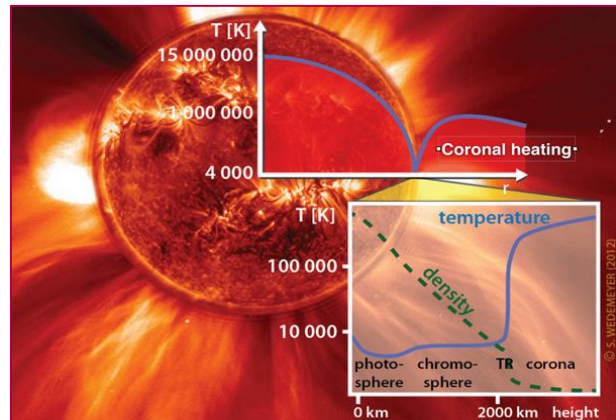


Figure 4. Gas temperature changes throughout the Sun

It is well known that gas temperature close to visible surface reaches its minimum, then rise again in thin layer – chromosphere and suddenly jump to millions of Kelvin in outermost layers (blue line). There were many attempts to solve so-called coronal heating problem during the last decades and now it remains one of the open questions in contemporary solar physics. The same can be said for the chromosphere, where the heating problem is even more unrecognized. A large number of heating mechanisms have been proposed for explanation of this problem. It is necessarily to provide accurate observations at high spatial, temporal and spectral resolution, facilitating the identification of the mechanisms responsible for the transport and dissipation of energy.

Due to the properties of the solar radiation at millimeter wavelengths, ALMA serves as a “quasi” thermometer, mapping narrow layers at different heights. It can measure the thermal structure and dynamics of the solar chromosphere and thus sources of atmospheric heating. Radio recombination and molecular lines (e.g., CO) potentially provide complementary kinetic and thermal diagnostics, while the polarization of the continuum intensity and the Zeeman effect can be exploited for valuable chromospheric magnetic field measurements.

The first regular observations of the Sun with ALMA have been carried out in December 2016 – April 2017.

<https://www.mn.uio.no/astro/english/research/projects/solaralma/>

2. SOLAR OBSERVATIONS IN CYCLE 5

ALMA modes, accessible in Cycle 5 solar observations:

- 3 most compact configurations: C43-1, C43-2, C43-3 (Baselines: 15-500 m)
- Only Band 3 and 6 pre-defined continuum setups.
- No full polarization.
- Special interferometric array comprising 12-m array and 7-m antennas.

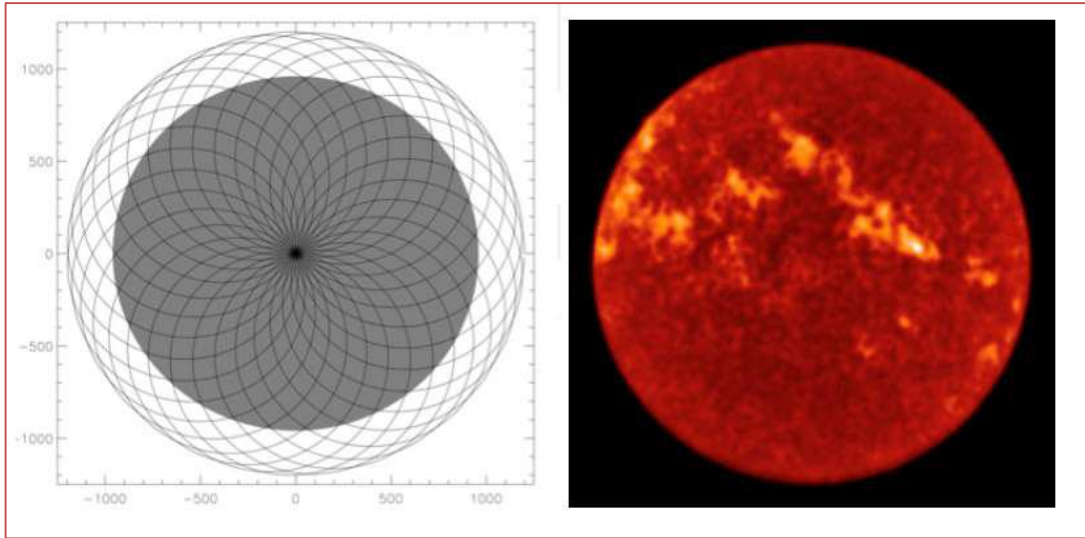


Figure 5. Circle scanning pattern of the Total Power array (left) used to obtain full disk maps of the Sun (right).

- e) Contemporaneous Total Power (TP) observations always included. (Fig. 5).

Double-circle scanning pattern, of the TP array can scan Solar disk in 7 minutes. (In presentation: <https://www.astro.uni-bonn.de/ARC/events/commdays2017/bonn/talks/ALMA Cycle5.pdf>).

3. SIMULATION OF PROMINENCE OBSERVATIONS IN ALMA

There are several examples of simulations of future ALMA observations of different solar structures based on ground-based observations. E.g. Heinzel et al. (2015) simulated the visibility of solar prominence in microwave and the detectability of their internal structures. First, it was necessary to find a prominence observed spectroscopically with high spatial resolution, where the fine structures are visible (see Fig. 6. and Fig. 7).

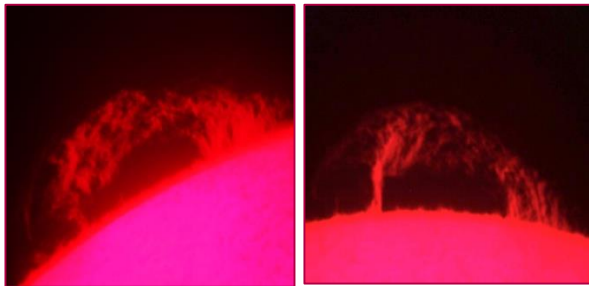


Figure 6. UWv/Large Coronagraph observations in the H α line: 09:28 UT (left) and 16:07 (right). (Adapted from Heinzel et al. 2015).

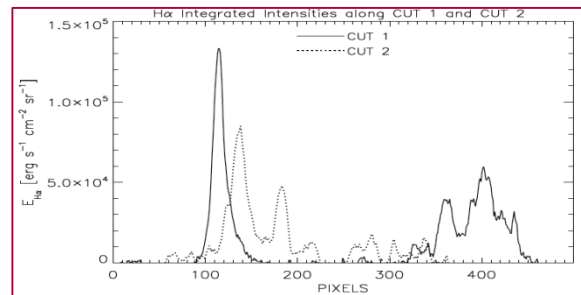
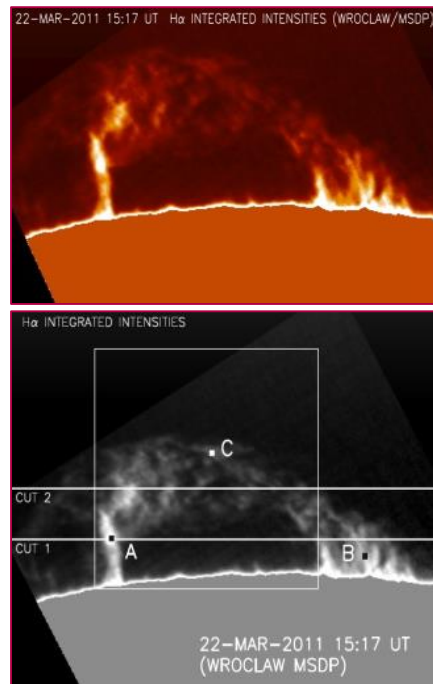


Figure 7. H α integrated intensities maps (upper) and cuts along two lines (lower) derived from Multichannel Subtractive Double Pass (MSDP) spectrograph (Mein 1991, Rompolt et al. 1993)

We used the H α coronagraphic MDSP spectral images (Mein 1991, Rompolt et al. 1993) of the prominence for the conversion into the microwave spectral images and see the possibility of prominence observations with ALMA. First, brightness temperature map of prominences was calculated using the relation between the emission measure (EM) of prominence plasma and the derived from observations integrated H α line intensities (Jejčić and Heinzel 2009). Using these methods, from future ALMA observations it will be possible to analyze the dynamics of the fine structures of prominences and get the temperature and other parameters of the plasma in cool prominence threads.

Next, standard CASA (Common Astronomy Software Applications, <http://casa.nrao.edu/>) package was used for simulations of ALMA prominence imaging. 3 mm (100 GHz) data corresponding to band 3 were chosen. H α data has a resolution of about 1'' only. For $\lambda = 1$ mm it's enough to have very compact ALMA array configuration. For $\lambda = 3$ mm the configuration of all fifty 12 m antennas is presented in Fig. 8. More extended ALMA configurations together with higher observing frequency can (and will) be used in future to reach resolution up to 0.005''.

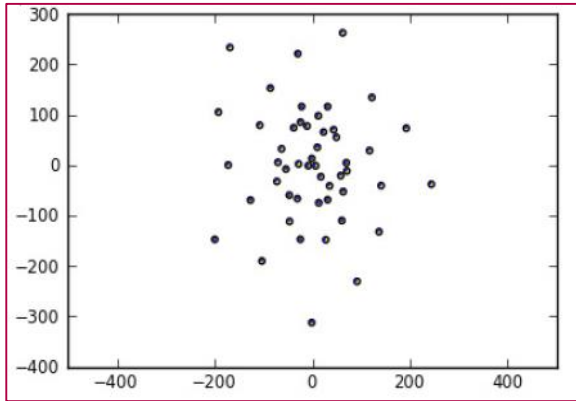


Figure 8. ALMA antennas configuration [axes are in meters] used for simulations of prominence observations in band 3.

Resulted simulated CASA mosaic pointings for the configuration shown in Fig. 8 is presented in Fig. 9. In total, 45 pointings were needed to cover the whole FOV with the prominence. The estimation was made using ALMA sensitivity calculator, the part of the ALMA OT package (ALMA Observing Tool, see: <http://almascience.eso.org/call-for-proposals/observing-tool>).

Simulated observing time is around 2 minutes, what is acceptable with respect to the characteristic dynamic time of prominence fine structures.

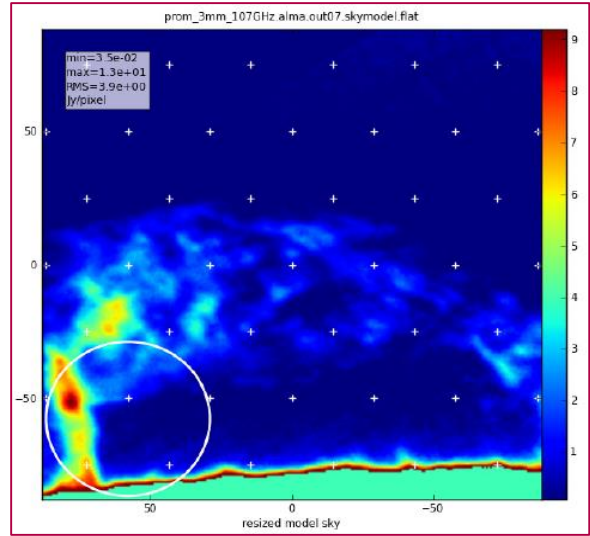


Figure 9. Simulated ALMA pointing centers (mosaic) overlaid on the background model radio map. Color scale is in units of Jy/pixel.

4. ALMA VISIBILITY OF COMPACT BURSTS

Another example concerns small compact brightenings (bursts) (CBs) observed in lower solar atmosphere. It was found that many such structures are visible in the optical or UV spectral range. In optical they are called Ellerman bombs (Ellerman 1917) and in ultraviolet as UV bursts - UVB. Although CBs are commonly observed in the solar atmosphere in many different spectral bands, their physics is still not well understood. These bursts are believed to be caused by small-scale magnetic reconnections in the low atmosphere (Georgoulis et al. 2002, Pariat et al. 2004, 2009, Zhao et al. 2017) that can heat the plasma and drive its flows. These phenomena appear mainly within solar active regions and display very intense, short-lived brightenings produced by plasma heated to temperatures of around 10^4 - 10^5 K (Peter et al. 2014). Therefore, they can be observed in the optical and UV spectral ranges. Fig. 10 presents an example of such compact bursts observed by Interface Region Imaging Spectrograph (IRIS) instrument (De Pontieu et al. 2014, Grubecka et al. 2016).

One of the most interesting aspects of CBs physics is the relation between EBs observed in the optical range and UVB observed in ultraviolet. We expect that ALMA observations will provide us some additional information and gives us a great opportunity to obtain a novel data, which can be used to confirm CBs location and their thermal structure in the solar atmosphere.

Since there are no previous radio observations of CBs, in order to be sure that CB structures will be observed by ALMA at 1 and 3 mm wavelengths (band 6 and 3), we performed preliminary simulations using the NLTE radiative transfer codes. We used three different "hot-spot" models of CBs adapted from Berlicki and Heinzel (2015). Model 1: CB in the chromosphere,

Model 2: CB around the temperature minimum region, Model 3: CB close to the photosphere - Fig. 11 (left). Then, using NLTE radiative transfer codes we determined their brightness temperature (T_B) in wavelengths corresponding to ALMA band 3 (3 mm) and 6 (1 mm), and for two other channels (6 mm and 0.45 mm), which can be used in future solar observations (Tab. 1).

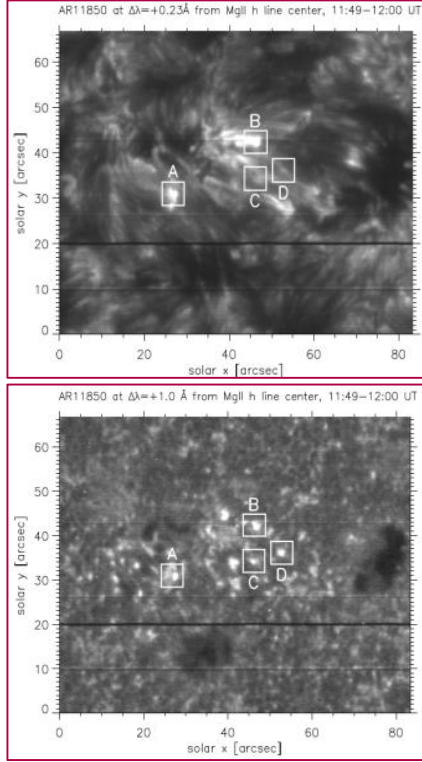


Figure 10. Example of UV bursts observations. Reconstructed monochromatic images of the AR 11850 observed by IRIS.

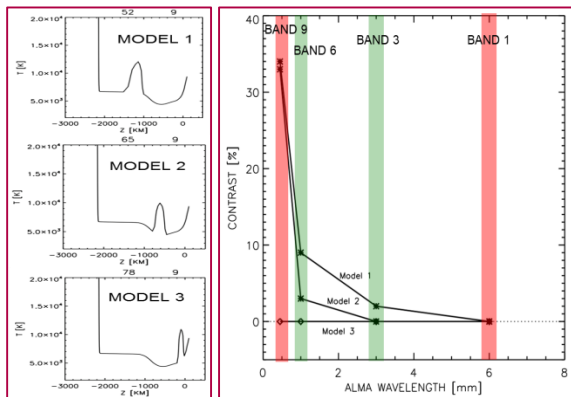


Figure 11. Representative "hot-spot" models used for NLTE calculation of CBs visibility in sub-mm/mm waves (left) and the simulated contrast for three models of CBs for different ALMA bands (right).

We compared the obtained T_B for all CBs (T_{CB}) with brightness temperature calculated for C7 model (Avrett & Loeser 2008) of the quiet-Sun atmosphere (T_{QS}). In

Fig. 11 (right) we present the theoretical brightness temperature contrast of CBs structures with respect to the quiet-Sun (QS) as a function of wavelength calculated for these three models of CBs. The contrast C is defined as:

$$C = (T_{CB} - T_{QS}) / T_{QS}, \quad (1)$$

where T_{CB} is the brightness temperature of CB observed at a given moment of time, and T_{QS} is the brightness temperature of the quiet-Sun atmosphere.

Model	$\lambda=0.45$ mm (band 9)	$\lambda=1$ mm (band 6)	$\lambda=3$ mm (band 3)	$\lambda=6$ mm (band 1)
C7 (QS)	$T_B=5370$ K $h_{[\tau=1]}=950$ km	$T_B=6330$ K $h_{[\tau=1]}=1100$ km	$T_B=6760$ K $h_{[\tau=1]}=1400$ km	$T_B=6810$ K $h_{[\tau=1]}=1520$ km
Hot-spot 52_9 1 (high chr.)	$T_B=7210$ K $h_{[\tau=1]}=1400$ km	$T_B=6930$ K $h_{[\tau=1]}=1620$ km	$T_B=6880$ K $h_{[\tau=1]}=1820$ km	$T_B=6790$ K $h_{[\tau=1]}=1890$ km
Hot-spot 65_9 2 (middle chr.)	$T_B=7130$ K $h_{[\tau=1]}=700$ km	$T_B=6500$ K $h_{[\tau=1]}=1140$ km	$T_B=6780$ K $h_{[\tau=1]}=1400$ km	$T_B=6810$ K $h_{[\tau=1]}=1520$ km
Hot-spot 78_9 3 (low chr.)	$T_B=5380$ K $h_{[\tau=1]}=350$ km	$T_B=6350$ K $h_{[\tau=1]}=1100$ km	$T_B=6770$ K $h_{[\tau=1]}=1400$ km	$T_B=6810$ K $h_{[\tau=1]}=1520$ km

Table 1. Brightness temperature and $\tau=1$ depth for given wavelength obtained from NLTE modeling.

From this plot and from Tab. 1 we can conclude that we will not see CBs if they are located in the photosphere (Model 3) because of very low contrast with respect to the quiet Sun. CBs located higher and higher should be progressively observed in shorter ALMA wavelengths, and CBs located in the chromosphere should be visible in almost all ALMA bands (except the 6 mm channel). Taking into account our previous results that CBs are located in the lower chromosphere we can see that some CBs will be visible by ALMA in band 3 and 6 and the visibility of CBs in different ALMA channels can give us important constraints on their formation altitude in the solar atmosphere.

5. SUMMARY

Simulated ALMA imaging – prominence mosaic: We have performed simulations of the brightness temperature of a quiescent prominence originally observed in the $H\alpha$ line and computed its visibility in mm range. By fitting the broadband ALMA spectra, one can derive both the kinetic temperature as well as the optical thickness. Simultaneous $H\alpha$ observations with high spatial resolution would also help to determine the optical thickness independently on the sub-mm/mm observations.

ALMA compact bursts visibility: Numerical simulations shows that compact brightenings (CBs) can be visible in different ALMA frequency bands. The computed brightness temperature T_B of CBs depends on the assumed model of the hot-spot and it is larger than the quiet-Sun value. The higher distance of the "hot-

spot" from the photosphere, the larger contrast of in all bands.

Solar observations of ALMA interferometer can significantly help us in understanding of different phenomena observed in lower solar atmosphere. However, one has to remember that ALMA observations can be even more valuable when obtained together with other observations of the chromosphere obtained e.g. with IRIS (in MgII lines), SDO (magnetograms, continuum images), and ground-based solar observatories in H α , Ca II H and K lines, He I 1083 nm, magnetic field maps, G-band, etc). Taken all these together, new results connected with fundamental questions about the Sun can be expected.

Acknowledgements

The work was supported by the project LM2015067. The work of AB was supported by grant No. 16-18495S of the Grant Agency of the Czech Republic and by the institutional grant RVO 67985815.

REFERENCES

- Avrett, E. H., Loeser, R.: 2008, ApJS, 175, 229
Berlicki, A., Heinzel, P., 2014, A&A, 567, 110
De Pontieu, B., Title, A.M., Lemen, J. R., et al.: 2014, Solar Phys., 289, 2733
Ellerman, F.: 1917, ApJ, 46, 298
Georgoulis, M. K., Rust, D. M., Bernasconi, P. N., Schmieder, B.: 2002, ApJ, 575, 506
Grubecka, M., Schmieder, B., Berlicki, A., Heinzel, P., Dalmasse, K., Mein, P.: 2016, A&A, 593, 32
Heinzel, P., Berlicki, A., Bartá, M., Karlický, Rudawy, P.: 2015, Solar Phys., 290, 1981
Jejčič, S., Heinzel, P. 2009, Solar Phys., 254, 89
Mein, P. 1991, A&A 248, 669
Pariat, E., Aulanier, G., Schmieder, B., et al.: 2004, ApJ, 614, 1099
Pariat, E., Masson, S., Aulanier, G.: 2009, ApJ, 701, 1911
Peter, H., Tian, H., Curdt, W., et al.: 2014, Science, 346, 1255726
Rompolt, B., Mein, P., Mein, N., Rudawy, P., and Berlicki, A. 1994, JOSO Annual Report 1993, ed. A. v. Alvensleben, pp. 87-91
Wedemeyer, S.: 2016, Space Sci. Rev. 200,1
Zhao, J., Schmieder, B., Li, H., Pariat, E., Zhu, X., Feng, L., Grubecka, M.: 2017, ApJ, 836, 52